Spontaneous emission from a two-level atom in anisotropic one-band photonic crystals: A fractional calculus approach

Jing-Nuo Wu,[1] Chih-Hsien Huang,[1] Szu-Cheng Cheng,[2,*] and Wen-Feng Hsieh[1,3,†]

[1]*Department of Photonics and Institute of Electro-Optical Engineering, National Chiao Tung University, Hsinchu, Taiwan, Republic of China*

[2]*Department of Physics, Chinese Culture University, Taipei, Taiwan, Republic of China*

[3]*Institute of Electro-Optical Science and Engineering, National Cheng Kung University, Tainan, Taiwan, Republic of China*

(Received 4 June 2009; revised manuscript received 30 October 2009; published 24 February 2010)

Spontaneous emission (SE) from a two-level atom in an anisotropic photonic crystal (PC) is investigated by the fractional calculus. Physical phenomena of the SE are studied analytically by solving the fractional kinetic equations of the SE. There is a dynamical discrepancy between the SE of anisotropic and isotropic PCs. We find that, contrary to the SE phenomenon of the isotropic PC, the SE near the band edge of an anisotropic PC shows no photon-atom bound state. It is consistent with the experimental results of Barth, Schuster, Gruber, and Cichos [Phys. Rev. Lett. **96**, 243902 (2006)] that the anisotropic property of the system enhances the SE. We also study effects of dispersion curvatures on the changes of the photonic density of states and the appearance of the diffusion fields in the SE.

DOI: 10.1103/PhysRevA.81.023827 PACS number(s): 42.50.Ct, 42.70.Qs, 32.80.Qk

I. INTRODUCTION

Photonic crystals (PCs), a new class of optical materials with periodic dielectric structures, provide a way to control the spontaneous emission (SE) through redistributing the photon density of states (DOS) near the photonic band gap (PBG). This control offers the key technology of manipulating light, such as in light emitting devices [1], quantum information processing [2], or solar cells [3]. The DOS near the band edge of PCs changes the optical behavior of an excited atom in a PC, such as the appearance of photon-atom bound states [4–8], spectral splitting [9], enhanced quantum interference [10], the coherent control of SE [11], non-Markovian effects [4–6,12], etc. Among these studies, the photon dispersion relation of a PC is described by the effective mass approximation [4,5], which leads to no photon DOS below the band edge frequency ω_c.

The dispersion relation near the band edge is assumed to be isotropic in early studies [4–7,9,12]. This isotropic PC system studied by John *et al*. [9,13] through using the Laplace transform method was predicted the presence of the unphysical bound state for the resonant atomic frequency lying outside the band gap. This unphysical bound state, corresponding to the prolonged lifetime effect in the experimental observation, was inconsistent with the experimental result that the prolonged lifetime effect would disappear when the emission peak lay outside the PBG region [14]. We resolved this inconsistency through using the fractional calculus method to solve the kinetic equation of the isotropic PC system and found no unphysical photon-atom bound state existing as the resonant atomic frequency lay in the allowed band [8]. This experimentally consistent result validated the correctness of applying the fractional calculus to this optical system.

In a practical three-dimensional PC with an allowed point-group symmetry, the photonic band structure is highly anisotropic, namely, the equal frequency surface near the band edge is no longer spherical. A vector form of photon dispersion relation is required to describe a more realistic anisotropy of the band. In this vector form of dispersion relation, the photon DOS is proportional to $\sqrt{\omega-\omega_c}$ while that of an isotropic dispersion relation is proportional to $1/\sqrt{\omega-\omega_c}$ [15], where ω stands for the eigenmode frequency and ω_c for the band edge frequency. This discrepancy of photon DOS will create different SE phenomena between anisotropic and isotropic PCs. The most prominent difference is the existence of diffusion field [16–19] in an anisotropic PBG. It was predicted theoretically by Yang *et al*. [16–19] that the bare atomic transition frequency lying above the band edge will be shifted into the forbidden gap by the interaction with the radiation modes where an atom-photon bound state is generated. In other words, the emitted photons tunnel through a PC for a localization length, and then reflect back, called Bragg reflection, to re-excite the atom. The emitter with frequency lying near band edge will not yield SE. Recently, Barth *et al*. observed experimentally [20] that the anisotropic properties of a PC could be detected by employing the CdSe on ZnS quantum dots (QDs) as emitters embedded inside artificial colloidal opals. When an emitter was placed inside a PC with the anisotropic band structure, the anisotropy would imprint on the SE of the system if the emission frequency lay in the forbidden gap. For the emission frequency of the QDs lying inside the forbidden gap, fluorescence and no SE from the QDs embedded inside colloidal opals with the strong and weak anisotropic band structure were observed, separately. There exists inconsistency between the experimental observation and previous theoretical studies, which predict no SE in the anisotropic PCs if the emitter's frequency lying inside the band gap. Experimental results showed the fundamental SE difference between the isotropic and anisotropic PCs. We believe that such a different SE is due to the dynamical discrepancy between the SE of anisotropic and isotropic PCs.

The SE behavior of the anisotropic PC system has also been studied by Kofman *et al*. [12] and John *et al*. [13,21,22]. Kofman *et al*. predicted that the anisotropic property would lead to the strong inhibition of the decaying behavior of the system. The result of John *et al*. exhibited a nonzero

*sccheng@faculty.pccu.edu.tw
†wfhsieh@mail.nctu.edu.tw

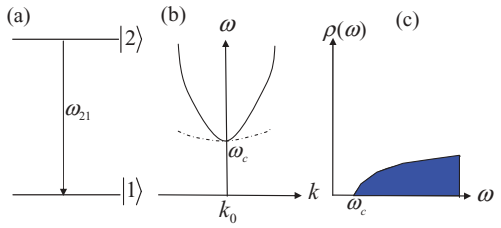

FIG. 1. (Color online) (a) A two-level atom with excited state $|2\rangle$ and ground state $|1\rangle$. The transition frequency ω_{21} is nearly resonant with the frequency range of the PBG reservoir. (b) Directional dependent dispersion relation near band edge with edge frequency ω_c. (c) DOS of the anisotropic one-band effective mass model.

excited-state population in the steady state for the atomic transition frequency lying near the band edge. Both conclusions are inconsistent with the experimental observation where anisotropy enhances the emission and no photon-atom bound state is observed if the emission frequency lies inside and near the band edge. In this paper, we study the dynamics of SE from a two-level atom embedded in a PC with anisotropic one-band model (Fig. 1). Fractional calculus, which was validated as a better mathematical method for studying the SE behavior of the atom-field interaction in PCs [8], is applied to solve the non-Markovian dynamics of the anisotropic optical system with threshold-like DOS. We find that the anisotropic property of the system enhances the SE of the system which agrees with the experimental observation by Barth *et al*. [20]. There still exist photon-atom bound states deep in the gap. The bound states, occurring near the band edge of the isotropic reservoir, become the decaying states in the anisotropic system. Such a change is due to there being less photon DOS, and then leading to the existence of the diffusion field near the band edge of the anisotropic PC. We also study effects of dispersion curvatures on the changes of the photonic density of states. The SE of the system with various curvatures of dispersion are solved by the fractional calculus and discussed on the basis of the curvature-dependent photon DOS and coupling strength.

The paper is organized as follows. In Sec. II, we show the basic SE theory of an atom in an anisotropic PC. Therein, the curvature dependent photon DOS and memory kernel referred to those derived by John *et al*. [13,21,22] are illustrated in Appendix A. In Sec. III, we solve the kinetic equation of the SE of an atom using the fractional calculus and express the analytical solution in terms of the fractional exponential function. The SE phenomenon of the anisotropic system is compared with that of the isotropic system. The spectral information of the anisotropic system consistent with the dynamical behavior is also addressed here based on the calculation presented in Appendix B. The new topic of the influence of curvature of the anisotropic dispersion relation on the dynamical behavior of the SE is discussed here as well. Finally, we summarize our results in Sec. IV.

II. BASIC THEORY OF A TWO-LEVEL ATOM IN AN ANISOTROPIC ONE-BAND PHOTONIC CRYSTAL

When the system of a two-level atom coupled to the field reservoir in a PC with anisotropic one-band model is considered, the Hamiltonian for this atom-field interacting system can be written as

$$H = \hbar\omega_{21}\sigma_{22} + \sum_{\vec{k}} \hbar\omega_{\vec{k}} a_{\vec{k}}^{\dagger} a_{\vec{k}} + i\hbar \sum_{\vec{k}} g_{\vec{k}} (a_{\vec{k}}^{\dagger}\sigma_{12} - \sigma_{21} a_{\vec{k}}), \tag{1}$$

where $\sigma_{ij} = |i\rangle\langle j|$ $(i, j = 1, 2)$ are the atomic operators for a two-level atom with excited state $|2\rangle$, ground state $|1\rangle$, and resonant transition frequency ω_{21}; $a_{\vec{k}}$ and $a_{\vec{k}}^{\dagger}$ are the annihilation and creation operators of the radiation field; $\omega_{\vec{k}}$ is the radiation frequency of mode $\vec{k}$ in the reservoir, and the atom-field coupling constant $g_{\vec{k}} = \frac{\omega_{21} d_{21}}{\hbar}[\frac{\hbar}{2\epsilon_0 \omega_{\vec{k}} V}]^{\frac{1}{2}} \hat{e}_{\vec{k}} \cdot \hat{u}_d$ is assumed to be independent of atomic position with the fixed atomic dipole moment $\vec{d}_{21} = d_{21}\hat{u}_d$. Here V is the sample volume, $\hat{e}_{\vec{k}}$ is the polarization unit vector of the reservoir mode $\vec{k}$, and ϵ_0 is the Coulomb constant. For simplicity, we consider one polarization direction for each mode $\vec{k}$.

In the single photon sector, the wave function of the system has the form

$$|\psi(t)\rangle = B(t)e^{-i\omega_{21}t}|2, \{0\}\rangle + \sum_{\vec{k}} C_{\vec{k}}(t)e^{-i\omega_{\vec{k}}t}|1, \{1_{\vec{k}}\}\rangle \tag{2}$$

with initial condition $B(0) = 1$ and $C_{\vec{k}}(0) = 0$. Here $B(t)$ labels the probability amplitude for the atom in its excited state $|2\rangle$ with an electromagnetic vacuum state and $C_{\vec{k}}(t)$ for the atom in its ground state $|1\rangle$ with a single photon in mode $\vec{k}$ with frequency $\omega_{\vec{k}}$. We got the equations of motion for the amplitudes by projecting the time-dependent Schrödinger equation on the one-photon sector of the Hilbert space as

$$\frac{d}{dt}B(t) = -\sum_{\vec{k}} g_{\vec{k}} C_{\vec{k}}(t) e^{-i\Omega_{\vec{k}}t}, \tag{3}$$

$$\frac{d}{dt}C_{\vec{k}}(t) = g_{\vec{k}} B(t) e^{i\Omega_{\vec{k}}t} \tag{4}$$

with detuning frequency $\Omega_{\vec{k}} = \omega_{\vec{k}} - \omega_{21}$. By substituting the time integration of Eq. (4) into Eq. (3), we have the time evolving equation of the excited-state probability amplitude

$$\frac{d}{dt}B(t) = -\int_0^t G(t-\tau)B(\tau)d\tau \tag{5}$$

with the memory kernel $G(t-\tau) = \sum_{\vec{k}} g_{\vec{k}}^2 e^{-i\Omega_{\vec{k}}(t-\tau)}$. This memory kernel is related to the dispersion relation of photon reservoir. For the anisotropic photonic band gap (PBG) reservoir, the dispersion relation has a vector form and could be expressed by the effective-mass approximation as [23]

$$\omega_{\vec{k}} \approx \omega_c + A(\vec{k} - \vec{k}_c)^2, \tag{6}$$

where $A \cong f\omega_c/k_c^2 = fc^2/\omega_c$ signifies different curvatures in different directions with scaling factor f whose value is in the order of unity and depends on the nature of the dispersion relation near the band edge ω_c. This anisotropic dispersion relation leads to the curvature-dependent photon DOS (see Appendix A)

$$\rho(\omega) = \frac{1}{4\pi^2}\sqrt{\frac{\omega-\omega_c}{A^3}}\Theta(\omega-\omega_c), \tag{7}$$

where $\Theta(x)$ is the Heaviside step function. This photon DOS has threshold-like behavior near band edge frequency ω_c which

results in the very different dynamical behavior of this atom-field interacting system from that of free space. The related memory kernel of the anisotropic system could be expressed as (see Appendix A)

$$G(t-\tau)=\frac{\omega_{21}^2 d_{21}^2}{4\epsilon_0\hbar}\int_0^\infty d\omega\frac{\rho(\omega)}{\omega}e^{-i(\omega-\omega_{21})(t-\tau)} \tag{8}$$

if we assume the direction of atomic dipole moment $\hat{u}_d$ is parallel to the polarization vector $\hat{e}_{\vec{k}}$. Substituting the photon DOS in Eq. (7) into this memory kernel, we obtain the memory kernel as

$$G(t-\tau)=\frac{\omega_{21}^2 d_{21}^2\sqrt{\omega_c}}{8\epsilon_0\hbar(\pi A)^{3/2}}e^{i(\Delta_c+\omega_c)(t-\tau)}\left\{\frac{e^{-i[\omega_c(t-\tau)+\pi/4]}}{\sqrt{\omega_c(t-\tau)}}\right.$$
$$\left.-\sqrt{\pi}[1-\Phi(\sqrt{i\omega_c(t-\tau)})]\right\}. \tag{9}$$

This full expression for memory kernel $G(t-\tau)$ is the same as that derived by John *et al.* in Ref. [22]. If $\omega_c(t-\tau)\gg 1$, we can asymptotically expand the error function $\Phi(x)$ to the second order, and the memory kernel becomes

$$G(t-\tau)=\frac{\beta^{1/2}/f^{3/2}}{\sqrt{\pi}(t-\tau)^{3/2}}e^{-i[3\pi/4-\Delta_c(t-\tau)]} \tag{10}$$

with the detuning frequency $\Delta_c=\omega_{21}-\omega_c$ of the atomic transition frequency ω_{21} from the band edge frequency ω_c and the coupling constant $\beta^{1/2}=(\omega_{21}^2 d_{21}^2\sqrt{\omega_c})/(16\pi\epsilon_0\hbar c^3)$ in units of $\mathrm{Hz}^{1/2}$. We will use this approximate memory kernel to investigate the SE behavior of the system because it is the approximate form of the full expression of memory kernel in Eq. (10) for $\omega_c(t-\tau)\gg 1$. This condition, $\omega_c(t-\tau)\gg 1$, could be satisfied for all but the $\tau=t$ point (as $\omega_c\approx 10^{15}$ Hz for optical transition), which would not affect the integral calculation of the SE probability as being omitted. Substituting this approximate memory kernel into the time evolving Eq. (5) and making the transformation $B(t)=e^{i\Delta_c t}D(t)$, we have the kinetic equation of this anisotropic system as

$$\frac{d}{dt}D(t)+i\Delta_c D(t)=\frac{\beta^{1/2}e^{i\pi/4}}{\sqrt{\pi}f^{3/2}}\int_0^t\frac{D(\tau)}{(t-\tau)^{3/2}}d\tau. \tag{11}$$

III. DYNAMICS OF SPONTANEOUS EMISSION

In this section, we will use fractional calculus to solve the kinetic equation of the anisotropic system and discuss the dynamics of SE on the basis of the obtained analytical solution. We have recently applied this approach to study the dynamics of SE from an atom embedded in a PC with an isotropic dispersion relation [8]. It was found that the dynamical behavior of SE from the optical systems with threshold-like photon DOS can be correctly and concisely described by fractional calculus.

When the right-hand side of the kinetic Eq. (11) is considered, we can express it as a Riemann-Liouville fractional differentiation operator [24–26] with order $\nu=1/2$. That is,

$$\int_0^t\frac{D(\tau)}{(t-\tau)^{3/2}}d\tau=\Gamma(-1/2)\frac{d^{1/2}}{dt^{1/2}}D(t) \tag{12}$$

with Gamma function $\Gamma(x)$. The kinetic equation thus has a fractional differential form as

$$\frac{d}{dt}D(t)+i\Delta_c D(t)+\frac{2\beta^{1/2}e^{i\pi/4}}{f^{3/2}}\frac{d^{1/2}}{dt^{1/2}}D(t)=0. \tag{13}$$

In order to solve this fractional kinetic equation, we manipulated the fractional operators including the integral operator (d^{-1}/dt^{-1}) and the fractional differentiation operator $d^{1/2}/dt^{1/2}$. Mathematically, the adopted manipulation is not unique provided that one could justify the function arrived at is the solution of the original fractional differential equation. The first step of our manipulation yields

$$D(t)-D(0)+i\Delta_c\frac{d^{-1}}{dt^{-1}}D(t)+\frac{2\beta^{1/2}e^{i\pi/4}}{f^{3/2}}\frac{d^{-1/2}}{dt^{-1/2}}D(t)=0. \tag{14}$$

The second step gives

$$\frac{d^{1/2}}{dt^{1/2}}D(t)+i\Delta_c\frac{d^{-1/2}}{dt^{-1/2}}D(t)+\frac{2\beta^{1/2}e^{i\pi/4}}{f^{3/2}}D(t)=\frac{t^{-1/2}}{\sqrt{\pi}}. \tag{15}$$

Here the initial condition $D(0)=B(0)=1$ has been applied. The probability amplitude $D(t)$ can be solved by performing the Laplace transform of the fractional derivatives including [26]

$$L\left[\frac{d^{1/2}}{dt^{1/2}}D(t)\right]=s^{1/2}\tilde{D}(s)-\left[\frac{d^{-1/2}}{dt^{-1/2}}D(0)\right]_{t=0}, \tag{16}$$

$$L\left[\frac{d^{-1/2}}{dt^{-1/2}}D(t)\right]=s^{1/2}\tilde{D}(s), \tag{17}$$

and

$$L[t^{-1/2}]=\frac{\Gamma(1/2)}{\sqrt{s}}, \tag{18}$$

where $\tilde{D}(s)$ is the Laplace transform of $D(t)$. These procedures give the Laplace transform of $D(t)$ as

$$\tilde{D}(s)=\frac{1}{s+i\Delta_c+2\beta^{1/2}e^{i\pi/4}s^{1/2}/f^{3/2}}. \tag{19}$$

In order to express this equation as a sum of partial fractions, we need to find the roots of the indicial equation $Y^2+2\beta^{1/2}e^{i\pi/4}Y/f^{3/2}+i\Delta_c=0$, where we have converted the variable $s^{1/2}$ into Y. There are two kinds of roots for this indicial equation: one with different roots $Y_1\neq Y_2$ and the other with degenerate root $Y_1=Y_2$. For the case of different roots, $\tilde{D}(s)$ could be expressed as

$$\tilde{D}(s)=\left(\frac{1}{(\sqrt{s}-Y_1)}-\frac{1}{(\sqrt{s}-Y_2)}\right)\frac{1}{(Y_1-Y_2)} \tag{20}$$

with

$$Y_1=e^{i\pi/4}\left(-\frac{\beta^{1/2}}{f^{3/2}}+\sqrt{\frac{\beta}{f^3}-\Delta_c}\right) \tag{21}$$

and

$$Y_2=e^{i\pi/4}\left(-\frac{\beta^{1/2}}{f^{3/2}}-\sqrt{\frac{\beta}{f^3}-\Delta_c}\right). \tag{22}$$

For the degenerate case, we have $\frac{\beta}{f^3} = \Delta_c$. The indicial equation becomes

$$Y^2 + 2\frac{\beta^{1/2}e^{i\pi/4}}{f^{3/2}}Y + \frac{\beta e^{i\pi/2}}{f^3} = 0 \tag{23}$$

or

$$\left(Y + \frac{\beta^{1/2}e^{i\pi/4}}{f^{3/2}}\right)^2 = 0. \tag{24}$$

The partial fractions of $\tilde{D}(s)$ can thus be written as

$$\tilde{D}(s) = \frac{1}{\left(\sqrt{s} + \frac{\beta^{1/2}e^{i\pi/4}}{f^{3/2}}\right)^2}. \tag{25}$$

The dynamical solution of the probability amplitude $D(t)$ can be obtained by applying the inverse Laplace transform on the partial-fractional forms of $\tilde{D}(s)$ for the two cases of different roots and degenerate root. The applied formulas of the inverse Laplace transform include

$$L^{-1}\left[\frac{1}{(\sqrt{s}-a)}\right] = E_t\left(-\frac{1}{2}, a^2\right) + aE_t\ (0, a^2) \tag{26}$$

and

$$L^{-1}\left[\frac{1}{(\sqrt{s}-a)^2}\right] = 2atE_t\left(-\frac{1}{2}, a^2\right) + (1+2a^2t) \times E_t\ (0, a^2) + aE_t\left(\frac{1}{2}, a^2\right) \tag{27}$$

with $E_t(\alpha, a) = t^\alpha \sum_{n=0}^{\infty} \frac{(at)^n}{\Gamma(\alpha+n+1)} = \frac{d^{-\alpha}}{dt^{-\alpha}}e^{at}$ being the two-parameter fractional exponential function of variable t, order α, and constant a [26]. The analytical solution for the fractional kinetic equation [Eq. (13)] of the anisotropic photonic crystal system is thus obtained. For $\beta/f^3 \neq \Delta_c$,

$$D(t) = \frac{1}{2e^{i\pi/4}\sqrt{\beta/f^3 - \Delta_c}}\left[Y_1^2 E_t\left(1/2, Y_1^2\right) - Y_2^2 E_t\left(1/2, Y_2^2\right) + Y_1 e^{Y_1^2 t} - Y_2 e^{Y_2^2 t}\right], \tag{28}$$

and for $\beta/f^3 = \Delta_c$,

$$D(t) = -2\frac{\beta^{3/2}e^{i3\pi/4}}{f^{9/2}}tE_t\left(\frac{1}{2}, i\beta/f^3\right) - \frac{\beta^{1/2}e^{i\pi/4}}{f^{3/2}}E_t\left(\frac{1}{2}, i\beta/f^3\right) + (1+2it\beta/f^3)e^{i\beta t/f^3} - 2\frac{\beta^{1/2}e^{i\pi/4}}{f^{3/2}}t^{1/2}/\sqrt{\pi}. \tag{29}$$

Here we have applied the relation of the fractional exponential function for special values $E_t(-1/2, a) = aE_t(1/2, a) + t^{-1/2}/\sqrt{\pi}$ and $E_t(0, a) = e^{at}$.

This analytical solution of Eq. (28) or Eq. (29), which has so far not been obtained, determines the dynamical behavior of the atomic excitation $B(t)$ and the amplitude of the radiation field which can be obtained via $B(t)$ in a standard way [18,27]. In this solution, the behavior of the indicial roots Y_1 and Y_2 depends on the lying region of the atomic transition frequency ω_{21} [see Eqs. (21) and (22)]. As the atomic frequency is in the higher-energy region $\omega_{21} > \omega_c + \beta/f^3$ ($\Delta_c > \beta/f^3$, region of allowed band), Y_1^2 and Y_2^2 are complex and the solution decays with time quickly. On the other hand, when the atomic frequency lies in the region $\omega_{21} < \omega_c + \beta/f^3$ ($\Delta_c < \beta/f^3$), the square of these roots, Y_1^2 and Y_2^2, is pure imaginary so that the dynamical solution in Eq. (28) contains nondecaying terms. These nondecaying terms oscillate individually with time and form atom-photon bound states as the atomic frequency lies deeply in the forbidden gap ($\omega_{21} \ll \omega_c$). Near band edge ($\omega_{21} \cong \omega_c$, $Y_1^2 \cong Y_2^2$), these nondecaying terms interfere with each other severely which leads to the decaying solution. This solution reveals that the anisotropic system exhibits decaying behavior as the atomic frequency lies in the region $\omega_{21} \leqslant \omega_c + \beta/f^3$ near band edge (including the allowed band edge and forbidden band edge) which agrees with the experimental observation in Ref. [20] where SE appeared with an extra angular anisotropy in the anisotropic PC system as the emission frequency of the embedded QDs lies in the forbidden gap. This result differs from that of the previous studies [16–19] by Zhu *et al.* whose discussion basis is the lying regions of the atomic transition frequency. They predicted that the bare atomic transition frequency lying in the region $\omega_{21} < \omega_c + \beta^{1/2}\omega_c^{1/2}$ will be shifted into the forbidden gap by the interaction with the radiation modes where a photon-atom bound state is generated. That is, there will not exist SE in the anisotropic PC system if the atomic transition frequency lies in the region either near the allowed band edge or near the forbidden band edge which disagrees with the experimental result in Ref. [20].

Instead of analyzing the integration contours for the probability amplitudes in previous solving procedures [16–19], we plot the dynamical behavior of this anisotropic system directly from our analytical solution of Eqs. (28) and (29) for $f = 1$. Based on the excited-state probability amplitude $P(t) = |B(t)|^2 = |D(t)|^2$, the dynamical behavior of the anisotropic system is shown in Fig. 2. It can be seen from Fig. 2 that typical characteristic of non-Markovian dynamics including nonexponential decay and atom-photon bound states exists

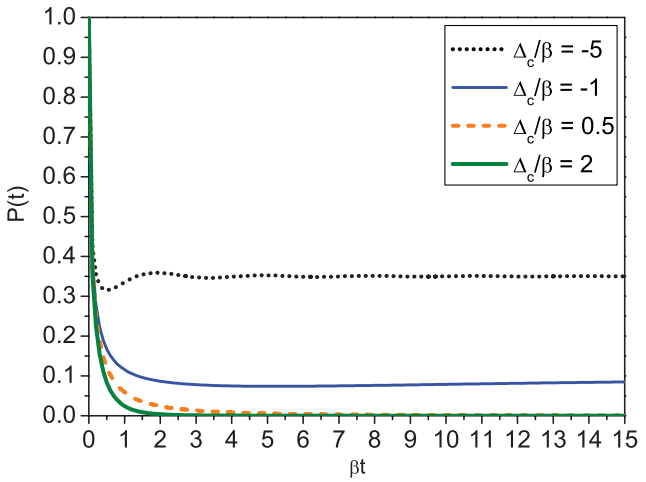

FIG. 2. (Color online) Dynamics of SE of the anisotropic PC system as a function of βt for several atomic detuning frequencies from the band edge in units of β, $\Delta_c/\beta = (\omega_{21} - \omega_c)/\beta$. Systems with positive atomic detuning frequencies $\Delta/\beta > 0$ have atomic frequencies lying within the allowed band while those with negative ones $\Delta/\beta < 0$ inside the PBG.

in the system which results from the special (threshold-like) DOS [Eq. (7)]. When the atomic transition frequency lies in the band gap ($\Delta_c < 0$), the system exhibits photon-atom bound states and decaying states in the allowed band ($\Delta_c > 0$). The dynamical behavior of the anisotropic system is almost the same as that of the isotropic system [8] except for the smaller probability of bound states and faster decaying behavior of decaying states. That is, the anisotropic property enhances the decaying behavior of this atom-field interacting system. This result is consistent with the experimental observation in Ref. [20] where SE appears only in anisotropic PC but not in the weak anisotropic PC system.

The physical reason of anisotropy enhancing decay can be obtained through comparing the difference of the anisotropic and isotropic PC systems. In these two systems, the most prominent difference is the behavior of photon DOS near band edge. The photon DOS is proportional to $1/\sqrt{\omega - \omega_c}$ for an isotropic PC system and $\sqrt{\omega - \omega_c}$ for an anisotropic system where ω and ω_c are the eigenmode frequency and band edge frequency. The singularity of photon DOS in isotropic system near band edge leads to the appearance of coherent propagating field while not large enough photon DOS in anisotropic system results in the coexistence of incoherent diffusion field and coherent propagating field. The energy transfer from the localized field to the diffusion field for the bound states of the anisotropic system leads to the smaller probability in the excited level. The coexisting energy of diffusion field and propagating field for decaying states results in faster decaying of the excited population. That is, anisotropy accompanied by not large enough DOS and the existence of diffusion field leads to the enhancement of decaying behavior of the bound states and decaying states near band edge.

The SE behavior of the anisotropic PC system could also be studied through the emission spectrum shown in Fig. 3. This figure is plotted according to Eq. (B9) where the definition of emission spectrum is based on the Wiener-Khintchine relation [21,22,28]. (see Appendix B) This spectrum exhibits no emission of radiation in the photonic band gap

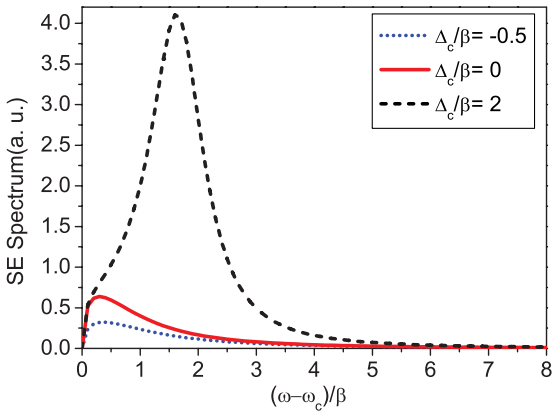

FIG. 3. (Color online) Emission spectra near an anisotropic band edge of a PC for several atomic detuning frequencies from the band edge in units of β, $\Delta_c/\beta = (\omega_{21} - \omega_c)/\beta$. Systems with positive atomic detuning frequencies $\Delta/\beta > 0$ have atomic frequencies lying within the allowed band while those with negative ones $\Delta/\beta < 0$ inside the PBG.

($\omega - \omega_c < 0$) and a Lorentzian shape throughout the allowed band ($\omega - \omega_c > 0$) because of the absence and abundance of photon DOS in these two regions. For the region near band edge ($\omega - \omega_c \to 0$), this spectrum shows non-Lorentzian shapes with fast increasing amount of emission. Since the photon DOS is a slowly increasing square root dependence of detuning frequency, we could deduce that this non-Lorentzian behavior of the spectrum stands for the existence of the diffusion field near band edge.

The SE behavior of a two-level atom embedded in an anisotropic PC has also been studied by Kofman *et al.* in Ref. [12] and John *et al.* in Refs. [13,21,22]. In Kofman's result, the relative peak value of the non-Lorentzian spectrum to the Lorentzian one (about 1/25) is smaller than ours (about 4/25). The appreciable values of the cut-off smoothing parameter, standing for the anisotropic property, result in the strong inhibition of the decaying behavior, which is inconsistent with the experimental observation of anisotropy enhancing the decaying behavior [12]. The work of Kofman *et al.* uses a different model of the photon DOS and that this model itself (but not its solution which is most likely correct) may be the reason of the discrepancy between their results and the experimental (and the present theoretical) results. On the other hand, John *et al.* observed that the dynamical SE exhibits a nonzero excited-state population for the atomic transition frequency lying within the gap which corresponds to an atom-photon bound state. This nonzero excited-state population exhibits larger values than those of our results. For example, as the atomic frequency lies in the gap of $\Delta_c/\beta = (\omega_{21} - \omega_c)/\beta = -5$, the non-zero value in John's result is 0.6 and 0.35 in ours. This value becomes 0.375 in John's and 0.075 in ours for $\Delta_c/\beta = -1$. The larger population for the bound states near band edge means that the SE can hardly occur as the emission frequency lies within the band gap which contradicts the experimental result.

The physical reason of the anisotropy enhancing the SE is further investigated in the following on the basis of the dynamical discrepancy of SE between the anisotropic and isotropic systems with the atomic transition frequency near band edge. In Fig. 4, we plot the dynamics of SE for these two systems with the atomic frequency lying close to the band edge. It reveals that states in the isotropic system exhibit bound ($\Delta_c < 0$) or slow decaying ($\Delta_c > 0$) behavior, whereas, in the anisotropic system, almost all of these states display fast decaying behavior. That is, the bound states close to the band edge of the isotropic system become the decaying states which lead to the appearance of SE in the anisotropic system. This result is consistent with the experimental observation in Ref. [20]. In order to investigate the local optical properties of PCs, Barth *et al.* doped the PCs of artificial colloidal opals with CdSe on ZnS core-shell quantum dots whose emission frequency lies inside the forbidden gap and the line width was narrower than the width of the band gap. They demonstrated that the characteristic patterns of fluorescence image from different quantum dots carried information on the modification of the optical mode density which arose from the direction-dependent photonic stop band. The anisotropic band structure of the artificial colloidal opals, which corresponds to the direction-dependent photonic stop band, brought an extra angular anisotropy of fluorescence image that was detected

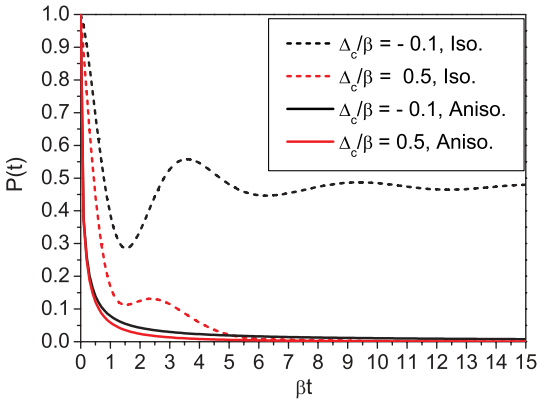

FIG. 4. (Color online) Dynamics of SE of the anisotropic (Aniso., solid lines) and isotropic (Iso., dashed lines) PC systems with atomic frequencies lying close to the band edge of PBG reservoir, $(\Delta_c/\beta = (\omega_{21} - \omega_c)/\beta \to 0)$. Systems with positive atomic detuning frequencies $\Delta/\beta > 0$ have atomic frequencies lying within the allowed band while those with negative ones $\Delta/\beta < 0$ inside the PBG.

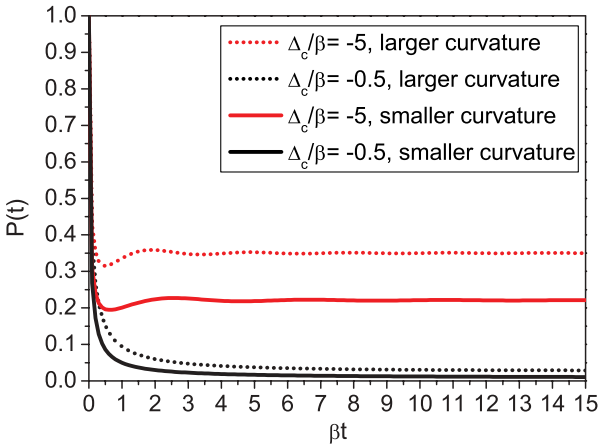

FIG. 5. (Color online) Dynamics of SE of the anisotropic PC systems with two kinds of curvatures in the dispersion relation. Solid lines for the system with smaller-curvature dispersion relation and dashed lines for the larger-curvature system. These systems have atomic frequencies lying within the PBG.

by defocused wide-field image of the single CdSe on ZnS quantum dots. These quantum dots did not emit light if they were embedded inside a PC with weak anisotropy of band structure. That is, SE appears only in the anisotropic PC as the emission frequency of the embedded quantum dots lies in the forbidden gap, but they did not emit light with bound states in the weak anisotropic PC system. Our results are validated by the presence of SE in the anisotropic PC which differs from the prediction of the previous studies [12,16–18,21,22]. Dynamical difference of the isotropic and anisotropic PC systems leads to the appearance of fluorescence image in the anisotropic system. Close to the band edge, photon DOS in the anisotropic case is nearly zero so that the incoherent diffusion field emerges to release some of the radiation energy. This diffusion field increases as the atomic frequency shifts to the band edge in the band gap and decreases as the frequency further shifts to the allowed band. The energy transferring from localized field to diffusion field reaches maximum at the band edge. The dynamical behavior of the two systems arriving at the great difference close to the band edge illustrates the existence of the diffusion field in the anisotropic system.

In Fig. 5, we show how the curvature of the dispersion relation affects the dynamical behavior of the anisotropic system which has so far not been explored. The solid lines are plotted for the system with the larger curvature ($f = 1$) of dispersion relation and dotted lines for the system with the smaller curvature ($f = 0.8$). For the bound states ($\Delta_c < 0$), the excited-state probability $P(t)$ of the system with the smaller curvature has the smaller value than that of the system with the larger curvature. On the other hand, the excited-state probability of the system with smaller curvature decays faster than that of the larger-curvature system for the decaying states ($\Delta_c > 0$). Without changing the units of energy (coupling constant β) and time ($1/\beta$), the dispersion relation of the smaller curvature has the larger DOS and coupling strength. As the atomic transition frequency moves from the band gap to the allowed band, this larger DOS leads to the earlier appearance of the diffusion field that corresponds to the earlier energy transfer from the localized field to the diffusion field for the bound states and earlier coexisting energy of the diffusion field and the propagating field for the decaying states. This earlier energy transfer and coexistence result in the smaller value of probability in the bound states and fast decaying in the decaying states along different wave vectors in the anisotropic system.

IV. CONCLUSION

We have used fractional calculus to solve the non-Markovian dynamics of the optical system consisting of a two-level atom coupled to a PBG reservoir with anisotropic one-band model. The dynamical SE shows that the anisotropic property enhances the decaying behavior of the states through the smaller probability of the photon-atom bound states ($\Delta_c < 0$) and the faster decaying rates for the decaying states ($\Delta_c > 0$). This theoretical result of anisotropy enhancing the decaying behavior is consistent with the experimental observation in Ref. [20] where SE happens only in the strong anisotropic PCs but not in the isotropic (weak anisotropic) system for the emission frequency lying in the forbidden gap. Investigating the dynamical difference between the isotropic and anisotropic systems, we found the reason of anisotropy enhancing decay originates from the the different photon DOS in the two systems and the existence of diffusion field in the anisotropic system. Not large enough DOS near band edge in the anisotropic system leads to the appearance of the incoherent diffusion field and energy transfer from the localized field to the diffusion field. The dynamical difference between the anisotropic and isotropic systems manifests itself more clearly as the atomic transition frequency lies close to the edge of the PBG reservoir. With the same atom-field coupling strength and detuning frequency in the forbidden gap, the bound states in the isotropic system turn into the unbound states in the anisotropic system. This change leads to the presence of SE in the anisotropic system that agrees with the experimental observation in Ref. [20]. The presence of SE in the anisotropic photonic crystal validates the correctness of our results while illustrates the inconsistency with the prediction

of the previous studies. The existence of the diffusion field in the anisotropic system is elucidated both by the large non-zero values of emission spectra near the band edge and the dynamical behavior of the two systems arriving at the great difference close to the band edge. We also investigated the topic of how the curvature of the anisotropic dispersion relation affects the dynamical behavior of the anisotropic system. Without changing the units of energy and time, the dispersion relation of the smaller curvature has larger DOS and coupling strength which leads to the earlier appearance of the diffusion field and energy transfer. This earlier energy transfer results in the smaller and faster-decaying probability along different wave vectors in the anisotropic PC system.

ACKNOWLEDGMENTS

We would like to gratefully acknowledge partial financial support from the National Science Council (NSC), Taiwan under Contract Nos. NSC-97-2811-E-009-023, NSC-96-2628-M-009-001-MY3, NSC-96-2112-M-034-002-MY3, and NSC-96-2628-M-009-001-MY3.

APPENDIX A: CALCULATION OF THE DENSITY OF STATES AND MEMORY KERNEL

We first derived the density of states for the anisotropic model in the effective-mass approximation, $\rho(\omega)$. The photon DOS, which counts the number of modes per unit volume available at a given frequency ω, can be written as

$$\rho(\omega) = \frac{1}{V}\sum_{\vec{k}} \delta(\omega - \omega_{\vec{k}}), \tag{A1}$$

where V is the quantization volume and one polarization direction for each mode $\vec{k}$ is considered. By introducing the anisotropic dispersion relation, $\omega_{\vec{k}} = \omega_c + A(\vec{k} - \vec{k}_c)^2$, and applying the continuum approximation, we can further express Eq. (A1) as

$$\rho(\omega) = \frac{1}{(2\pi)^3}\int_0^\infty d\vec{k}\delta[\omega - \omega_c - A(\vec{k} - \vec{k}_c)^2]. \tag{A2}$$

Here we assume a fixed orientation of the atomic dipole moment under the electric dipole approximation. Making the substitution of $\vec{q} = \vec{k} - \vec{k}_c$ and performing the angular integration, we obtained the photon DOS as

$$\rho(\omega) = \frac{1}{4\pi^2}\sqrt{\frac{\omega - \omega_c}{A^3}}\Theta(\omega - \omega_c), \tag{A3}$$

which was articulated in Eq. (7) of the text.

We then calculated the memory kernel for this anisotropic system. Starting from the definition of memory kernel below Eq. (5) and inserting a δ function, we had the memory kernel

$$\begin{aligned} G(t-\tau) &= \sum_{\vec{k}} g_{\vec{k}}^2 e^{-i(\omega_{\vec{k}} - \omega_{21})(t-\tau)} \\ &= \int_0^\infty d\omega\delta(\omega - \omega_{\vec{k}})\sum_{\vec{k}} g_{\vec{k}}^2 e^{-i(\omega-\omega_{21})(t-\tau)} \end{aligned} \tag{A4}$$

with $g_{\vec{k}}^2 = [\omega_{21}^2 d_{21}^2(\hat{e}_{\vec{k}}\cdot\hat{u}_d)^2]/(2\epsilon_0\hbar\omega_{\vec{k}}V)$. If we assumed $\hat{e}_{\vec{k}}\cdot\hat{u}_d = 1$ (the direction of atomic dipole moment $\hat{u}_d$ is parallel to the polarization vector $\hat{e}_{\vec{k}}$) and considered the definition of photon DOS in Eq. (A1), the memory kernel became

$$G(t-\tau) = \frac{\omega_{21}^2 d_{21}^2}{4\epsilon_0\hbar}\int_0^\infty d\omega\frac{\rho(\omega)}{\omega}e^{-i(\omega-\omega_{21})(t-\tau)}. \tag{A5}$$

By substituting the photon DOS in Eq. (A3) and applying the integral formula $\int_0^\infty dx(x^2 e^{-b^2x^2})/(x^2+a^2) = \sqrt{\pi}/2b - ae^{a^2b^2}\pi[1-\Phi(ab)]/2$ with the error function $\Phi(x) = (2/\sqrt{\pi})\int_0^x dte^{-t^2}$ [29], we obtained the memory kernel as

$$\begin{aligned} G(t-\tau) = \frac{\omega_{21}^2 d_{21}^2\sqrt{\omega_c}}{8\epsilon_0\hbar(A\pi)^{3/2}}e^{i(\Delta_c+\omega_c)(t-\tau)}\Bigg\{&\frac{e^{-i[\omega_c(t-\tau)+\pi/4]}}{\sqrt{\omega_c(t-\tau)}} \\ &- \sqrt{\pi}[1-\Phi(\sqrt{i\omega_c(t-\tau)})]\Bigg\}. \end{aligned} \tag{A6}$$

This full expression of memory kernel was listed in Eq. (9) of the text where the coefficient before the error function was $\sqrt{\pi}$ instead of $\sqrt{\pi}/2$ in the result of John *et al.* in Ref. [21]. As we expanded the error function asymptotically to second order, it gave

$$\begin{aligned} 1-\Phi(\sqrt{i\omega_c(t-\tau)}) = \frac{1}{\pi}e^{-i\omega_c(t-\tau)}\Bigg\{&\frac{\sqrt{\pi}}{\sqrt{i\omega_c(t-\tau)}} \\ &- \frac{\sqrt{\pi}/2}{[i\omega_c(t-\tau)]^{3/2}}\Bigg\}, \end{aligned} \tag{A7}$$

which was valid for $\omega_c(t-\tau) \gg 1$. This asymptotic expansion of the error function led to the asymptotic memory kernel

$$G(t-\tau) \cong \frac{\omega_{21}^2 d_{21}^2}{16\epsilon_0\hbar(A\pi)^{3/2}\omega_c}\frac{e^{-i[3\pi/4-\Delta_c(t-\tau)]}}{(t-\tau)^{3/2}}. \tag{A8}$$

This neat form of memory kernel could be obtained only if the valid coefficient $\sqrt{\pi}/2$ was in front of the error function. It could be further expressed as the form of Eq. (10) shown in the text

$$G(t-\tau) = \frac{\beta^{1/2}/f^{3/2}}{\sqrt{\pi}(t-\tau)^{3/2}}e^{-i[3\pi/4-\Delta_c(t-\tau)]}, \tag{A9}$$

if we defined the coupling constant $\beta^{1/2} = (\omega_{21}^2 d_{21}^2\sqrt{\omega_c})/(16\pi\epsilon_0\hbar c^3)$. Here the phase factor $e^{-i3\pi/4}$ was the same as those obtained by John *et al.* in recent works of Refs. [13,22] but different from that in earlier work of Ref. [21].

APPENDIX B: CALCULATION OF THE EMISSION SPECTRUM

The emission spectrum of the anisotropic PC system has been studied by Kofman *et al.* [12] and John *et al.* [22]. However, apparent inconsistency existed between their results and with the experimental observation by Barth *et al.* [20]. For example, John *et al.* observed a long spectral tail that extended far into the allowed electromagnetic continuum for all atomic detunings near the band edge while Kofman saw a much weaker nonexponential tail. Besides, The relative amount of emitted radiation in John's result for the atomic frequency at band edge to that in the allowed band (about 1/3) was much larger than that obtained by Kofman (about 1/25). In order to illuminate the effect of the anisotropy on the PC system, we calculate the emission spectrum of the system again.

The emission spectrum of the system $S(\omega)$ was defined by the ensemble average of the correlation function of the excited-state probability amplitude $B(t)$ through the Wiener-Khintchine relation as [21,22,28]

$$S(\omega) \equiv \int_{-\infty}^{\infty} e^{i(\omega-\omega_{21})\tau} \langle B(\tau)B(0)\rangle d\tau + \text{c.c.}, \tag{B1}$$

where $\langle \ldots \rangle$ stands for the ensemble average and c.c. for the complex conjugate of the leading term. If we used the initial condition $B(0) = 1$ and assumed the ensemble average was stationary, which meant independent of time, this spectrum could be written as

$$\begin{aligned} S(\omega) &= 2\text{Re}\left\{\int_{-\infty}^{\infty} e^{i(\omega-\omega_{21})\tau} B(\tau) d\tau\right\} \\ &= 2\text{Re}\{\tilde{B}[s = -i(\omega-\omega_{21})]\} \end{aligned} \tag{B2}$$

with $\text{Re}\{\ldots\}$ standing for the real part of the function and $\tilde{B}(s)$ being the Laplace transform of $B(t)$. This Laplace transform $\tilde{B}(s)$ could be obtained through applying the Laplace transformation to the time evolving equation

$$\frac{dB(t)}{dt} = -\int_0^t G(t-\tau)B(\tau)d\tau. \tag{B3}$$

It gave

$$\tilde{B}(s) = \frac{1}{s + \tilde{G}(s)} \tag{B4}$$

with $\tilde{G}(s)$ being the Laplace transform of the memory kernel, i.e.,

$$\tilde{G}(s) \equiv \frac{\omega_{21}^2 d_{21}^2}{4\epsilon_0 \hbar} \int_0^{\infty} dt \left[e^{-st} \int_0^{\infty} d\omega \frac{\rho(\omega)}{\omega} e^{-i(\omega-\omega_{21})t}\right]. \tag{B5}$$

When the anisotropic photon DOS [Eq. (7)] is considered, this memory kernel became

$$\tilde{G}(s) = \frac{\omega_{21}^2 d_{21}^2}{8A^{3/2}\pi^2\epsilon_0\hbar} \int_0^{\infty} d\omega \frac{\sqrt{\omega}}{(\omega+\omega_c)(s+i\omega-i\Delta_c)} \tag{B6}$$

with the detuning frequency $\Delta_c = \omega_{21} - \omega_c$. The complex integral in the memory kernel can be dealt by the calculus of residues [30], which gave

$$\tilde{G}(s) = \frac{4\omega_c \beta^{1/2}}{f^{3/2}} \frac{e^{i3\pi/4}}{\sqrt{s-i\Delta_c} + \sqrt{i\omega_c}} \tag{B7}$$

with $\beta^{1/2} = (\omega_{21}^2 d_{21}^2 \sqrt{\omega_c})/(16\pi\epsilon_0\hbar c^3)$ and $f = A\omega_c/c^2$. Substituting this memory kernel into Eq. (B4) and using the relation $\tilde{B}(\omega) = \tilde{B}\,[s = -i(\omega-\omega_{21})]$, we obtained the expression of $\tilde{B}(\omega)$. For $\omega > \omega_c$,

$$\begin{aligned} \tilde{B}(\omega) = \frac{(\omega/\omega_c)}{\omega_c} \Bigg\{ &\frac{4}{f^{3/2}} \sqrt{\frac{\beta}{\omega_c}} \sqrt{\left(\frac{\omega}{\omega_c}\right) - 1} - i\left(\frac{\omega}{\omega_c}\right) \Bigg[\left(\frac{\omega}{\omega_c}\right) \\ &- 1 - \left(\frac{\Delta_c}{\omega_c}\right) + \frac{4}{f^{3/2}} \sqrt{\frac{\beta}{\omega_c}} \Big/ \left(\frac{\omega}{\omega_c}\right)\Bigg]\Bigg\}^{-1}, \end{aligned} \tag{B8}$$

and for $\omega < \omega_c$,

$$\begin{aligned} \tilde{B}(\omega) = \frac{i}{\omega_c} \Bigg\{ &\left(\frac{\omega}{\omega_c}\right) - 1 - \left(\frac{\Delta_c}{\omega_c}\right) \\ &+ \frac{4}{f^{3/2}} \sqrt{\frac{\beta}{\omega_c}} \Big/ \left[\sqrt{1 - \left(\frac{\omega}{\omega_c}\right)} + 1\right]\Bigg\}^{-1}. \end{aligned} \tag{B9}$$

Taking the real part of $\tilde{B}(\omega)$, we got the emission spectrum

$$S(\omega) \propto \sqrt{\frac{\beta}{\omega_c}} \frac{2b\left(\frac{\omega}{\omega_c}\right)\sqrt{\left(\frac{\omega}{\omega_c}\right) - 1}}{b^2\left(\frac{\omega}{\omega_c} - 1\right)(\beta/\omega_c) + \left(\frac{\omega}{\omega_c}\right)^2\left[\left(\frac{\omega}{\omega_c}\right) - 1 - \left(\frac{\Delta_c}{\omega_c}\right) + b\sqrt{\frac{\beta}{\omega_c}} \Big/ \left(\frac{\omega}{\omega_c}\right)\right]^2} \Theta\left(\frac{\omega}{\omega_c} - 1\right) \tag{B10}$$

with $b = 4/f^{3/2}$. This emission spectrum differed from that obtained by John *et al*. in Ref. [22] with one more frequency dependent factor (ω/ω_c) in the numerator. This factor appeared naturally as the phase factor $e^{i3\pi/4}$ was merged into the denominator of the Green function. In Fig. 3, the emission spectrum was plotted for several atomic detuning frequencies Δ_c/β with $f = 1$. We saw the spectrum exhibited the Lorentzian behavior throughout the allowed band $(\omega - \omega_c > 0)$ with exponentially decaying tail, which was the same as that observed by Kofman *et al*. [12]. This Lorentzian spectrum elucidated the atom-field interaction in this region to be Markovian as in free space. As expected, the spectrum showed no emission of radiation in the region of photonic band gap $(\omega - \omega_c < 0)$ because of the lack of the photon density of modes. Between these two extremes, near the allowed band edge $(\omega - \omega_c \to 0)$, the system exhibited fast increasing amount of emission illustrating the existence of the diffusion field. Photon DOS of the anisotropic system increased slowly with the square root detuning frequency from band edge in this region, i.e., $\rho(\omega) \propto \sqrt{\omega - \omega_c}$. Emission from the coherent propagating field occupying these few DOS was relatively little compared with that from the field without photon DOS, named incoherent diffusion field. Diffusion field existed in this anisotropic system was thus elucidated by the fast increasing amount of emission near band edge. When the relative amount of the emitted radiation from systems with different atomic detuning frequencies $(\Delta_c/\beta = (\omega_{21} - \omega_c)/\beta)$ was considered, we observed that our result had values between those of John's and Kofman's. For example, this relative value was (4/25) for emission from system with the atomic detuning frequency at the band edge $(\Delta_c/\beta = 0)$ to that in the allowed band $(\Delta_c/\beta = 2)$, larger than that by

Kofman *et al*. (1/25) and smaller that by John *et al*. (2/3) [22]. The larger value than that of Kofman's result illustrated again that anisotropy of the system enhanced the decaying behavior. The agreement between our spectral and dynamical SE was interpreted by the smaller value than that of John's result.

[1] L. Chen and A. V. Nurmikko, Appl. Phys. Lett. **85**, 3663 (2004).
[2] N. Vats and T. Rudolph, J. Mod. Opt. **48**, 1495 (2001).
[3] S. Nishimura, N. Abrams, B. A. Lewis, L. I. Halaoui, T. E. Mallouk, K. D. Benkstein, J. van de Lagemaat, and A. J. Frank, J. Am. Chem. Soc. **125**, 6306 (2003).
[4] S. John and J. Wang, Phys. Rev. Lett. **64**, 2418 (1990).
[5] S. John and J. Wang, Phys. Rev. B **43**, 12772 (1991).
[6] S. John and T. Quang, Phys. Rev. Lett. **78**, 1888 (1997).
[7] S. Bay, P. Lambropoulos, and K. Molmer, Phys. Rev. Lett. **79**, 2654 (1997).
[8] S.-C. Cheng, J.-N. Wu, M.-R. Tsai, and W.-F. Hsieh, J. Phys. Condens. Matter **21**, 015503 (2009).
[9] S. John and T. Quang, Phys. Rev. A **50**, 1764 (1994).
[10] S. Y. Zhu, H. Chen, and H. Huang, Phys. Rev. Lett. **79**, 205 (1997).
[11] T. Quang, M. Woldeyohannes, S. John, and G. S. Agarwal, Phys. Rev. Lett. **79**, 5238 (1997).
[12] A. G. Kofman, G. Kurizki, and B. Sherman, J. Mod. Opt. **41**, 353 (1994).
[13] M. Woldeyohannes and S. John, J. Opt. B: Quantum Semiclass. Opt. **5**, R43 (2003).
[14] M. Fujita, S. Takahashi, Y. Tanaka, T. Asano, and S. Noda, Science **308**, 1296 (2005).
[15] S. John and T. Quang, Phys. Rev. Lett. **74**, 3419 (1995).
[16] S.-Y. Zhu, Y. Yang, H. Chen, H. Zheng, and M. S. Zubairy, Phys. Rev. Lett. **84**, 2136 (2000).
[17] Y. Yang, M. Fleischhauer, and S.-Y. Zhu, Phys. Rev. A **68**, 022103 (2003).
[18] Y. Yang, M. Fleischhauer, and S.-Y. Zhu, Phys. Rev. A **68**, 043805 (2003).
[19] Y. Yang, G. Li, H. Chen, and S.-Y. Zhu, Opt. Commun. **265**, 559 (2006).
[20] M. Barth, R. Schuster, A. Gruber, and F. Cichos, Phys. Rev. Lett. **96**, 243902 (2006).
[21] N. Vats and S. John, Phys. Rev. A **58**, 4168 (1998).
[22] N. Vats, S. John, and K. Busch, Phys. Rev. A **65**, 043808 (2002).
[23] S. John, Phys. Rev. Lett. **58**, 2486 (1987).
[24] K. B. Oldham and J. Spanies, *Fractional Calculus* (Academic Press, New York, 1974).
[25] S. G. Samko, A. A. Kilbas, and O. I. Marichev, *Fractional Integrals and Derivatives: Theory and Applications* (Gordon and Breach, London, 1993).
[26] K. S. Miller and B. Ross, *An Introduction to the Fractional Calculus and Fractional Differential Equations* (Wiley, New York, 1993).
[27] M. O. Scully and M. S. Zubairy, *Quantum Optics* (Cambridge University Press, Cambridge, 1997).
[28] W. H. Louisell, *Quantum Statistical Properties of Radiation* (John Wiley and Sons, Inc., New York, 1973).
[29] I. S. Gradshteyn and I. M. Ryzhik, *Tables of Integrals, Series and Products* (Academic Press, New York, 1980).
[30] P. M. Morse and H. Feshbach, *Methods of Theoretical Physics* (McGraw-Hill, Inc., New York, 1994).